Generation and control of polarization-entangled photons from GaAs island quantum dots by an electric field

Mohsen Ghali[1,†], Keita Ohtani[1], Yuzo Ohno[1] & Hideo Ohno[1,2]

Semiconductor quantum dots are potential sources for generating polarization-entangled photons efficiently. The main prerequisite for such generation based on biexciton–exciton cascaded emission is to control the exciton fine-structure splitting. Among various techniques investigated for this purpose, an electric field is a promising means to facilitate the integration into optoelectronic devices. Here we demonstrate the generation of polarization-entangled photons from single GaAs quantum dots by an electric field. In contrast to previous studies, which were limited to In(Ga)As quantum dots, GaAs island quantum dots formed by a thickness fluctuation were used because they exhibit a larger oscillator strength and emit light with a shorter wavelength. A forward voltage was applied to a Schottky diode to control the fine-structure splitting. We observed a decrease and suppression in the fine-structure splitting of the studied single quantum dot with the field, which enabled us to generate polarization-entangled photons with a high fidelity of 0.72 ± 0.05.

The generation and the manipulation of on-demand entangled photons are crucial in the emerging fields of quantum cryptography[1] and quantum computation[2]. Hence, single semiconductor quantum dots (QDs) are considered potential sources of polarization-entangled photons through the radiative decay of biexcitons; a QD is initially excited to the biexciton state, and then it decays by a cascaded emission of two photons[3]. When the two exciton intermediate states are degenerate, the polarizations of the two photons are maximally entangled. However, they are not typically degenerated via the fine-structure splitting (FSS) owing to the asymmetries in the QD confining potential[4], and its FSS energy (Δ_{FSS}) must be less than the radiative linewidth (Γ). It is also necessary that the cascade emission takes place with a high probability, which is expected to increase the visibility of the two-photon coincidence and the degree of entanglement[5]. Until now, the sources that use this scheme have been limited to In(Ga)As QDs[6–12] (with Γ of a few μeV)[13], but the elongated shape and the strain in these QD systems induce a large in-plane anisotropy and a sizable Δ_{FSS} (10–100 μeV)[14]. Because the typical Δ_{FSS} observed for a QD exciton is usually larger than Γ, techniques to decrease Δ_{FSS} must be used[13,15–17].

Here we take a different approach that satisfies these requirements by using the naturally bright[4,18,19] island QDs, made of a narrow GaAs quantum well (QW) with a monolayer thickness fluctuation[4,20]; the FSS is suppressed by applying an electric field (E) in the forward direction onto a Schottky diode structure. In addition to the lack of strain, which affects Δ_{FSS}, GaAs island QDs provide an oscillator strength that is one order of magnitude larger than that of self-assembled In(Ga)As QDs; hence, they present a higher emission probability[17,19,21] with a large Γ (23 μeV)[4]. This result arises because GaAs island QDs have a greater lateral extent area of the exciton than In(Ga)As QDs. Theoretically, GaAs island QDs are also expected to exhibit a smaller Δ_{FSS} than In(Ga)As QDs because of the small electron–hole exchange energy, which is one order of magnitude smaller than that of self-assembled InAs QDs[22]. We observed a clear reduction of Δ_{FSS} and a rotation of the exciton polarization axis caused by the electric field. At a certain value of the electric field, where Δ_{FSS} is suppressed to below our detection limit, we obtained a high circular polarization degree of the exciton photoluminescence (PL) under a circularly polarized excitation. The polarization-dependent photon correlation measurements showed that applying electric fields to GaAs QDs makes it possible to manipulate the two-photon polarization state from the polarization-correlated state to the polarization-entangled state.

Results

GaAs island QDs in a Schottky device. GaAs QDs were grown on an n-GaAs (100) substrate by molecular beam epitaxy. The QDs were created in the regions of one monolayer thicker than the other regions, which were formed during a 2-min growth interruption on both sides of the GaAs QW. Figure 1a,b shows the fabricated Schottky diode structure and the simulation of the band diagram, respectively. No cavity structure was used to enhance the light-collection efficiency. An independent time-resolved μ-PL measurement was performed where the excitonic lifetime was found to be less than 300 ps, which reflects the fast radiative emission from our GaAs dots. We applied a forward bias voltage between the top gate metal contact and the bottom n-GaAs substrate (see Methods). The forward bias current (I) is quite small ($I < 5$ nA) owing to the presence of a thick $Al_{0.3}Ga_{0.7}As$ barrier, which inhibits large currents from flowing through the device (Fig. 1c). Low temperature ($T = 4$ K) PL spectra are shown in Figure 1d as a function of E. The excitation and collection of PL was conducted through a 200-nm metal aperture, which was opened by electron beam lithography. For all measurements, we selected the excitation wavelength of 735–740 nm, which is about 40–50 meV higher than the exciton emission energy (approximately one longitudinal optical phonon energy of GaAs).

Such an excitation wavelength is suitable to efficiently supply the photo-generated carriers to the QDs via phonon scattering.

Photoluminescence under applied electric fields. The exciton PL emissions from two representative dots (dot A and dot B as indicated in Fig. 1d) were observed with their redshift in the presence of the electric field. Here we focused on the result of dot A, where four emissions—an exciton (X), biexciton (XX), negatively charged exciton (X^-) and positively charged exciton (X^+)—were detected. In addition to the linear and the superlinear responses of their PL intensities to the excitation power, the exciton and the biexciton emissions were assigned according to their opposite linear polarization (Fig. 1e). Thus, the exciton and the biexciton can be easily distinguished from X^- and X^+. The PL intensity dropped by 45% when E increased from 0 to 29.2 kV cm^{-1}, most probably owing to an increase of the field-assisted carrier tunnelling. Above E = 29.2 kV cm^{-1}, the PL became significantly weak and broadened, which makes it difficult to determine Δ_{FSS} at E > 30 kV cm^{-1} (at these fields, I increases progressively above 10 nA (Fig. 1c)). The observed dependence of the PL spectra on the electric field for other dots was similar to that represented in Figure 1d.

Changes in polarization and FSS with the electric field. The in-plane asymmetry of GaAs QDs is reflected in the polarization anisotropy exhibited by the integrated PL spectra of the exciton and the biexciton. By carefully following the evolution of the exciton and the biexciton PL energies with the polarization angle, we obtained a clear behaviour that could be fitted with a sinusoidal function, from which we extracted Δ_{FSS}. The polarization axis of the PL was determined by the angle that represents the maximum splitting energy, and Δ_{FSS} was measured with an accuracy of 2–3 μeV. Figure 2a shows a clear nonlinear change of Δ_{FSS} with the electric field, where Δ_{FSS} decreased from 38 μeV at E=0 to below our detection limit when the field approached 30 kV cm^{-1}. We studied five quantum dots; three of them showed a similar FSS suppression behaviour with the increase in the electric field. Moreover, on tuning Δ_{FSS} over the measured range of the electric field, we observed a clear rotation of the exciton polarization axis. Figure 2b summarizes the relationship between the electric field and φ, which describes the orientation of the exciton polarization axis relative to the crystal axis [1$\overline{1}$0]. We found that as the field increased, the exciton polarization axis continuously rotated from $\varphi = 90°$, where it aligned with the crystal axis [110] at E = −45 kV cm^{-1}, until it approached 45°, and it became independent of the polarization axis at E = 29.2 kV cm^{-1}, where Δ_{FSS} was minimized within our detection limit (Fig. 2c). Similar results have recently been reported for InAs/GaAs QDs using a large electric field of up to a few hundred kV cm^{-1} (ref. 12).

To confirm that Δ_{FSS} approaches zero with the increase in the electric field, the QD exciton was excited by circularly polarized light with an energy of 40 meV above the exciton PL transition energy, and the exciton spin polarization was monitored by its PL circular polarization. Such one-longitudinal optical-phonon-assisted circularly polarized excitation induces a coherent superposition of both fine structure components of the exciton, which are split by Δ_{FSS}. Analogous to the well-known Hanle effect, the degree of the exciton PL circular polarization (P_c) is expected to increase when Δ_{FSS} approaches zero[23]. Figure 2d shows the evolution of P_c with the electric field. The polarized spectra of the exciton were plotted in Figure 2e for two different electric field strengths (E = 23 and 29.2 kV cm^{-1}). When the field strength increased, a strong increase in P_c (65%) was observed, indicating that Δ_{FSS} was greatly reduced at E = 29.2 kV cm^{-1} compared with that at E = 23 kV cm^{-1}.

Quantum-confined Stark spectroscopy. Now, we discuss the influence of the electric field on Δ_{FSS} based on the QD exciton and biexciton Stark shift. A quantum confined Stark effect can introduce
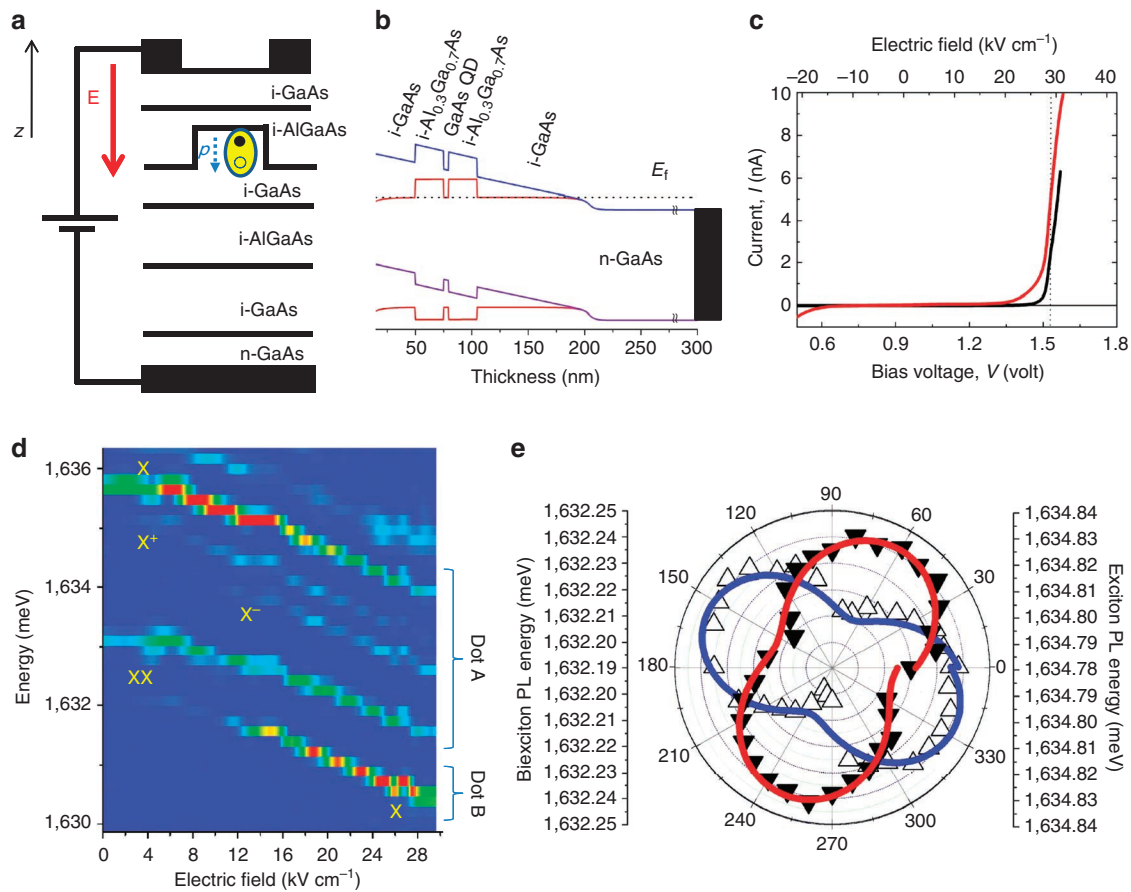
Figure 1 | Fabricated Schottky diode structure and QD photoluminescence characteristics on applying an electric field. (**a**) Schematics of the fabricated diode structure (not to scale). The thick red arrow denotes the direction of the applied vertical electric field E. The black arrow points to the sample growth direction z. The dotted arrow refers to the directional polarity of the QD exciton dipole moment p, and the yellow oval represents the hole component of the wavefunction below the electron in the dot. (**b**) One-dimensional simulation results of the device band alignment with the electric field (E = −45 kV cm^{-1}) for the blue line and (E = 0 kV cm^{-1}) for the red line. (**c**) I − V characteristics of the Schottky device in darkness (black line) and under 735 nm laser illumination (red line); the vertical dashed line refers to E = 29.2 kV cm^{-1} (where I = 5 nA). (**d**) Evolution of the photoluminescence spectra of two different GaAs quantum dots (dot A and dot B) with the electric field. For dot A, the recombination of the neutral exciton (X), the positively charged exciton (X^+), the negatively charged exciton (X^-) and the biexciton (XX) is shown. (**e**) Polar plot of the exciton (open-up triangles) and the biexciton (closed-down triangles) PL energies with the linear polarization angles, measured relative to [1$\bar{1}$0], the sample's crystallographic axis, at E = 18 kV cm^{-1}. The solid blue (red) lines represent a fit to the exciton (biexciton) data, respectively, with a sinusoidal function, from which the fine-structure splitting magnitude and the exciton polarization direction were extracted.

changes in the QD Coulomb interactions by modifying the overlap of the carriers' wavefunctions. Experimentally, we found that the emissions exhibited a quadratic shift according to the equation $E_{PL}(E) = E_{PL}^0 + pE + \beta E^2$, where E_{PL} is the PL energy, and p and β are the permanent dipole and the polarizability of the state, respectively[24]. The solid lines in Figure 3 show the results of the parabolic fit to the exciton and biexciton emission energies, from which we extracted $p/e = -0.28 \pm 0.02$ nm and $\beta = -1.32 \pm 0.008$ µeV/(kVcm^{-1})^2 for the exciton. A negative value of p indicates a permanent dipole moment along the $-z$ direction; the hole wavefunction is located below the electron wavefunction (Fig. 1a).

In Figure 3, we plotted the electric-field dependence of the biexciton binding energy B_{XX}, which is defined as the energy difference between the exciton and the biexciton emissions. A systematic reduction in B_{XX} was observed. In a simple model, B_{XX} can be expressed as: $B_{XX} = (-2J_{eh} + J_{ee} + J_{hh})$, where J_{eh} is the electron–hole Coulomb interaction, and J_{ee} and J_{hh} are the electron–electron and the hole–hole Coulomb interactions, respectively. At E = 0, a small spatial separation between the electron and the hole wavefunctions exists, giving rise to a permanent dipole moment. Because positive E and p are in the same direction as depicted in Figure 1a, the wavefunc-

tion separation increased with an increasing electric field, which led to a reduction in B_{XX} by decreasing J_{eh}. A decrease in B_{XX} with the reduction of Δ_{FSS} was previously reported for annealed InAs self-assembled QDs[25]. Although further study is required to understand the B_{XX} reduction with the field, our results suggest that a positive electric field manipulates the electron–hole separation along the growth direction, and simultaneously modifies their lateral confinement; thus, the electric field enables the exciton dipole to rotate in the sample plane. Modulation of the exciton wavefunction by the electric field results in a decrease in the QD electron–hole overlap and a nonlinear change in the long-range component of the electron–hole exchange interaction, which strongly influences the FSS[26]. Although the electron–hole separation is expected at negative fields, we observed a sizable value of Δ_{FSS} (= 60 µeV) at E < − 30 kV cm^{-1} (Fig. 2b), indicating the absence of a significant lateral modification of the exciton wavefunction at such field strengths. This observation is consistent with the lack of in-plane rotation of the exciton dipole within this electric field range (Fig. 2b,c). The polarity dependence may be related to the asymmetric nature of the two confining interfaces in our GaAs island QD[27]. It should be noted that the electric field dependence of Δ_{FSS} in this case is qualitatively different from
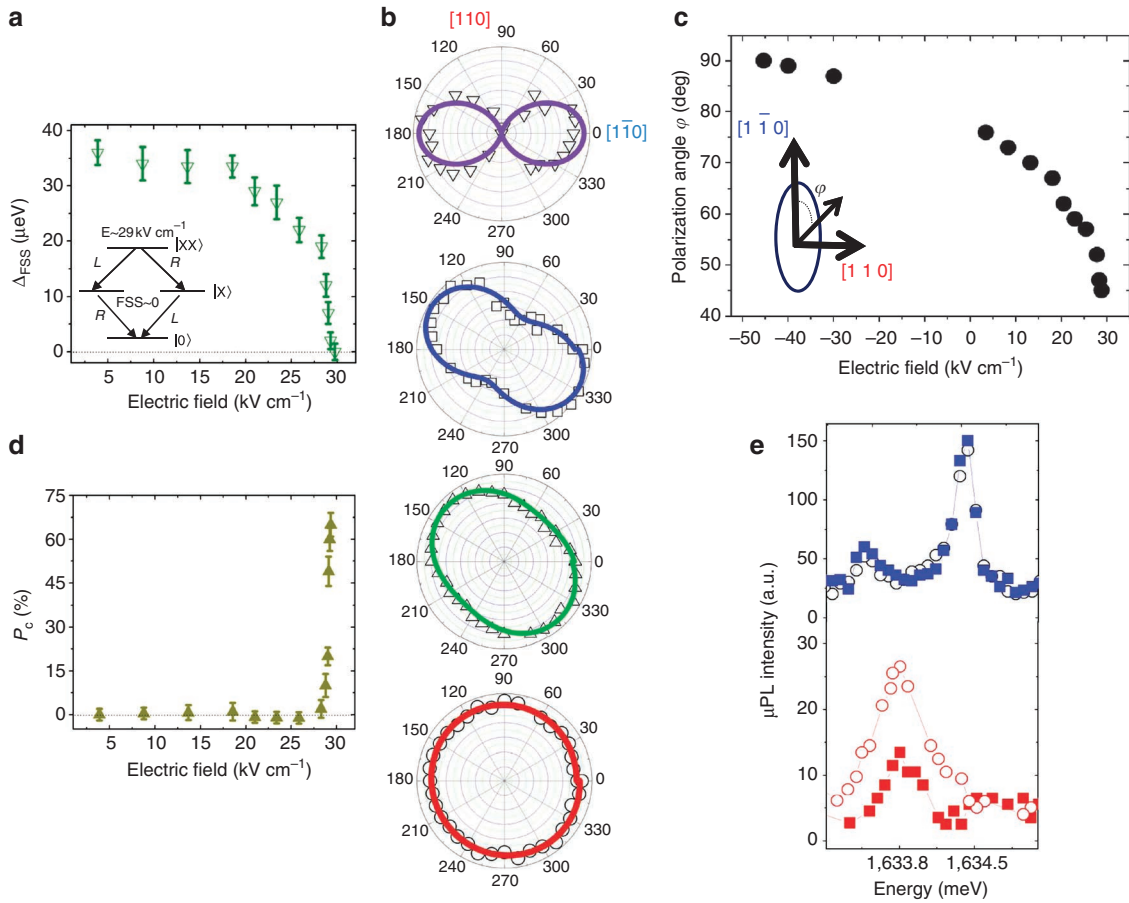
3

Figure 2 | Electric field-dependence of fine-structure splitting energy and QD exciton polarization. (**a**) Variation of Δ_{FSS} (closed-down triangles) with the electric field. The inset shows a sketch of the biexciton–exciton cascaded emission for E~29 kV cm^{-1} (Δ_{FSS}~0). (**b**) Linear polarization dependence of the exciton X at various electric fields (from top): E = −45, 22, 27 and 29.2 kV cm^{-1}, relative to [1$\bar{1}$0], the sample's crystallographic axis. All polar plots have an axis scale increment of 10 µeV. The solid lines represent a fit to the data with a sinusoidal function. (**c**) Variation of the exciton polarization angle φ with the electric field. The inset describes the angle φ relative to the crystal axis [1$\bar{1}$0]. The exciton PL emission cannot be seen when −30 < E < −0.2 kV cm^{-1}. (**d**) Evolution of the degree of exciton PL circular polarization P_c (closed-up triangles) with the electric field. (**e**) Circular polarization resolved detection σ^+ (open-circles) and σ^- (closed-squares) of the exciton PL spectra at two different electric fields: 23 kV cm^{-1} (top) and 29.2 kV cm^{-1} (bottom).

that of InAs/GaAs QDs, in which Δ_{FSS} decreases linearly with the application of large reverse electric fields[12]. This difference might result from the 'weak'[4,28] lateral confining potential of our GaAs island QDs compared with the 'strong' lateral confinement of InAs/GaAs QDs (as a result, the carriers' wavefunctions in GaAs island QDs will be more sensitive to the applied electric fields than those of InAs/GaAs QDs).

Polarization-resolved photon correlation measurements. The suppression of the FSS by the electric field enabled us to examine the generation of polarization-entangled photons from the same dot. This generation relies on the biexciton–exciton cascaded emission, which can proceed along two paths as shown in the inset of Figure 2a: with a left-circularly-polarized (L) biexciton photon followed by a right-circularly-polarized (R) exciton photon, or vice versa. As Δ_{FSS} approaches 0, it is impossible to distinguish which path has been followed, and the two photons should be emitted in the Bell state: $[(|R_{XX}L_X\rangle+|L_{XX}R_X\rangle)]/\sqrt{2}$. Alternatively, the Bell state can be rewritten[1,9] in the linear polarization basis as $[(|H_{XX}H_X\rangle+|V_{XX}V_X\rangle)]/\sqrt{2}$ or in the diagonal polarization basis as $[(|D_{XX}D_X\rangle+|D'_{XX}D'_X\rangle)]/\sqrt{2}$. The first clear signature of the polarization-entangled photons from our GaAs island dot was observed in polarization-resolved photon correlation measurements (Fig. 4a). A clear photon bunching occurred for the collinearly
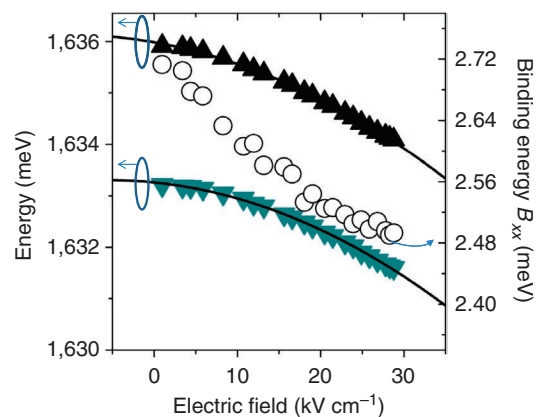

Figure 3 | Results of Stark spectroscopy measurements. PL peak positions of the exciton (closed-up triangles) and the biexciton (closed-down triangles) with the electric field. The electric field dependence of the biexciton binding energy (B_{XX}), which is defined as the energy difference between the exciton and the biexciton emissions, is also shown and indicated by open circles. The left scale corresponds to the exciton and the biexciton data, and the right scale corresponds to the B_{XX} data; both scales are referred to by arrows. The solid lines represent the parabolic fits to the data, from which p and β are extracted.
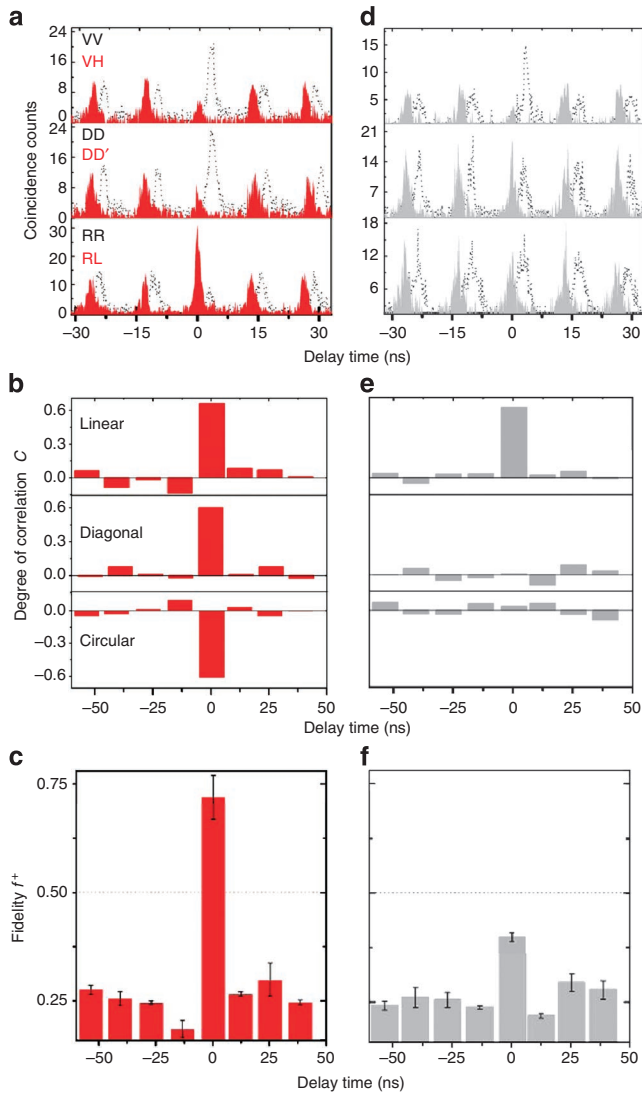
Figure 4 | Second-order cross-photon correlation histograms of biexciton–exciton photons. (**a**) Exciton and biexciton coincident counts for $E = 29.2\,kV\,cm^{-1}$ ($\Delta_{FSS} \sim 0$) as a function of the delay time. The black dotted lines represent the coincident counts measured for photons of the same polarization, and the solid red lines show the orthogonal polarizations. (**b**) Degree of correlation C at $E = 29.2\,kV\,cm^{-1}$ for the linear (top), the diagonal (middle) and the circular (bottom) bases. (**c**) Fidelity f^+ for several central pulse periods at $E = 29.2\,kV\,cm^{-1}$. (**d**) Exciton and biexciton coincident counts for $E = 18\,kV\,cm^{-1}$ ($\Delta_{FSS} = 30\,\mu eV$) as a function of the delay time. The black dotted lines represent the coincident counts measured for photons of the same polarizations, and the solid grey lines show the orthogonal polarizations. (**e**) Degree of correlation C at $E = 18\,kV\,cm^{-1}$ for the linear (top), the diagonal (middle) and the circular (bottom) bases. (**f**) Fidelity f^+ for several central pulse periods at $E = 18\,kV\,cm^{-1}$. The QD was excited quasi-resonantly by the 740 nm laser energy to minimize the recapture of the carriers into the dot. The black dotted histograms in **a** and **d** are time-shifted for clarity. The top, the middle and the bottom panels in **a** and **d** show the coincident counts measured in the linear, the diagonal and the circular basis angles, respectively: H, horizontal; V, vertical; D, diagonal; D' orthodiagonal; R, right; L, left. The averaged accumulation times for the histograms measured at $E = 18$ and $29.2\,kV\,cm^{-1}$ were 160 and 200 min, respectively.

polarized exciton and the biexciton photons emitted in the same cascade at zero delay time in the linear (VV) and the diagonal bases (DD), whereas in the circular basis, the bunching was observed only for the counter-circularly polarized (RL) photons. This result

is expected for entangled photon pairs in the Bell state because the two-photon wavefunctions can be expressed as a superposition of the collinearly, co-diagonally or cross-circularly-polarized photon pairs[3]. The degree of entanglement was quantified using the degree of correlation (see Methods) (Fig. 4b), where the entanglement fidelity f^+ of the emitted photons projected onto the maximally entangled state was determined directly by combining the correlations measured in the linear, the diagonal and the circular polarization bases[29]. We found that the peak at the zero time delay yields a fidelity $f^+ = 0.72 \pm 0.05$ (Fig. 4c) without any background light subtraction, which exceeds the threshold of 0.5 for a source emitting classically polarization-correlated states. Thus, the result proves that entangled photons were generated. Figure 4d depicts the results of the polarization-resolved photon correlation measurements when the electric field decreased to $18\,kV\,cm^{-1}$, where the corresponding Δ_{FSS} was $30\,\mu eV$. Under these conditions, there is a high probability of generating a pair of photons with the same linear polarization, as shown in Figure 4e. No significant polarization correlation was observed in the diagonal and the circular bases. Hence, the fidelity under these conditions is below 0.5 (Fig. 4f), which shows that the two-photon state at $18\,kV\,cm^{-1}$ is classically polarization correlated.

Discussion
The above results demonstrate that the two-photon state emitted from the same GaAs QD can be manipulated from the polarization-correlated state to a polarization-entangled state by applying a vertical electric field. Because these GaAs island QDs emit light at a short wavelength (~750 nm), they will be useful for efficient detection of photons with silicon detectors. The reduction in Δ_{FSS} for these dots, caused by the forward bias voltage, may also allow the fabrication of an efficient visible light-emitting diode, which can emit entangled photons with a high emission probability that is suitable for qubit-based optical[30] and spin[31] quantum computation applications.

Methods
Quantum dots and device fabrication. The sample consists of a 14-monolayer GaAs QW sandwiched between 25-nm-thick $Al_{0.3}Ga_{0.7}As$ barriers and covered with a 50-nm-thick GaAs cap layer. A 2-min growth interruption was performed on both sides of the GaAs QW. This QW structure was grown on top of a 100-nm-thick undoped GaAs layer deposited on a 300-nm-thick n-GaAs layer ($n = 1.5 \times 10^{17}\,cm^{-3}$). All layers were epitaxially grown by molecular beam epitaxy on an n-GaAs (100) substrate, which was used as a backside electrode. A Ti/Au film with an aperture of 200 nm in diameter was deposited on the sample surface to form a Schottky contact. The electric field is defined as $E = (V_g - V_0)/d$, where V_g is the applied gate voltage, V_0 is the Schottky barrier height (= 0.93 V) obtained from independent photocurrent measurements, and d is the distance between the sample surface and the bottom n-doped GaAs layer ($d = 205\,nm$).

Optical spectroscopy measurements. We focused the laser and collected the luminescence using a microscope objective lens with a numerical aperture of 0.4. A continuous wave and pulsed (6 ps) $Ti:Al_2O_3$ laser was used for the excitation. The PL spectra were analysed by using a 55-cm-long monochromator coupled to an N_2-cooled silicon charge-coupled device detector. A spectral notch filter was used to suppress the laser emission. Most of the QDs across the sample had line widths of ~120 μeV and were limited mainly by our set-up resolution. In the photon correlation measurements, the Hanbury Brown and Twiss (HBT) set-up was used to generate the photon correlation histograms with various polarization combinations. The collected PL was divided into two orthogonal detection arms using a 50/50 nonpolarizing pellicle beam splitter. Each arm of the HBT set-up was equipped with a single monochromator to filter the PL emission individually, in addition to a high-sensitivity avalanche photodiode. The electrical pulses from the two avalanche photodiodes were used to start and to stop a time-to-amplitude converter. The data within ± 2.5 ns of $g^{(2)}_{XX,X}(\tau)$ were integrated to extract the total number of counts. For all optical measurements, the sample temperature was $T = 4\,K$. A combination set of half-wave and quarter-wave plates was inserted in the collection path of the HBT set-up for proper polarization state selection. No background subtraction or filtering was performed. The fidelity f^+ to the Bell state was calculated by measuring the correlation function

$$C(\tau) = \frac{g^{(2)}_{XX,X}(\tau) - g^{(2)}_{XX,\bar{X}}(\tau)}{g^{(2)}_{XX,X}(\tau) + g^{(2)}_{XX,\bar{X}}(\tau)}$$

for each polarization basis of the linear, diagonal and circular types[29], where $g_{XX,X}^{(2)}(\tau)$ and $g_{XX,\bar{X}}^{(2)}(\tau)$ are the second-order correlation functions when a biexciton photon is detected with a co-polarized and a cross-polarized exciton photon, respectively. The f^+ is expressed as:

$$f^+ = \frac{1}{4}(1 + C_{\mathrm{linear}} + C_{\mathrm{diagonal}} - C_{\mathrm{circular}})$$

where C_{linear}, C_{diagonal} and C_{circular} are the degrees of polarization correlation between the two emitted photons in the linear, the diagonal and the circular bases, respectively.

References

1. Gisin, N., Ribordy, G., Tittel, W. & Zbinden, H. Quantum cryptography. *Rev. Mod. Phys.* **74,** 145–195 (2002).
2. Chen, J. *et al.* Demonstration of a quantum controlled NOT-gate in the telecommunication band. *Phys. Rev. Lett.* **100,** 133603 (2008).
3. Benson, O. *et al.* Regulated and entangled photons from a single quantum dot. *Phys. Rev. Lett.* **84,** 2513–2516 (2000).
4. Gammon, D. *et al.* Fine structure splitting in the optical spectra of single GaAs quantum dots. *Phys. Rev. Lett.* **76,** 3005–3008 (1996).
5. Santori, C. *et al.* Polarization-correlated photon pairs from a single quantum dot. *Phys. Rev. B* **66,** 045308 (2002).
6. Stevenson, R. M., Young, C. K., Atkinson, P., Ritchie, D. A. & Shields, A. J. A semiconductor source of entangled photon pairs. *Nature* **439,** 179–182 (2006).
7. Akopian, N. *et al.* Entangled photon pairs from semiconductors quantum dots. *Phys. Rev. Lett.* **96,** 130501 (2006).
8. Hafenbrak, R. *et al.* Triggered polarization-entangled photon pairs from a single quantum dot up to 30 K. *New J. Phys.* **9,** 315–324 (2007).
9. Mohan, A. *et al.* Polarization-entangled photons produced with high-symmetry site-controlled quantum dots. *Nature Photon.* **4,** 302–306 (2010).
10. Salter, C. L. *et al.* An entangled-light-emitting diode. *Nature* **465,** 594–597 (2010).
11. Dousse, A. *et al.* Ultrabright source of entangled photon pairs. *Nature* **466,** 217–220 (2010).
12. Bennett, A. J. *et al.* Electric-field-induced coherent coupling of the exciton states in a single quantum dot. *Nature Phys.* **6,** 947–950 (2010).
13. Mar, J. D. *et al.* Electrical control of fine-structure splitting in self-assembled quantum dots for entangled photon pair creation. *Appl. Phys. Lett.* **97,** 221108 (2010).
14. Seguin, R. *et al.* Size-dependent fine structure splitting in self-organized InAs/GaAs quantum dots. *Phys. Rev. Lett.* **95,** 257402 (2005).
15. Stevenson, R. M. *et al.* Magnetic field induced reduction in the exciton polarization splitting in InAs quantum dots. *Phys. Rev. B* **73,** 033306 (2006).
16. Seidl, S. *et al.* Effect of uniaxial stress on excitons in a self-assembled quantum dot. *Appl. Phys. Lett.* **88,** 203113 (2006).
17. Marcet, S., Ohtani, K. & Ohno, H. Vertical electric field tuning of the exciton fine structure splitting and photon correlation measurements of GaAs quantum dot. *Appl. Phys. Lett.* **96,** 101117 (2010).
18. Gust, J. R. *et al.* Measurement of optical absorption by a single quantum dot exciton. *Phys. Rev. B* **65,** 241310(R) (2002).
19. Hours, J., Senellart, P., Peter, E., Cavanna, A. & Bloch, J. Exciton radiative lifetime controlled by the lateral confinement energy in a single quantum dot. *Phys. Rev. B* **71,** 161306(R) (2005).
20. Brunner, K. *et al.* Sharp-line photoluminescence and two-photon absorption of zero-dimensional biexcitons in a GaAs/AlGaAs structure. *Phys. Rev. Lett.* **73,** 1138–1141 (1994).
21. Gammon, D. *et al.* Homogeneous linewidth in the optical spectrum of a single gallium arsenide quantum dot. *Science* **273,** 87–90 (1996).
22. Luo, J. W., Bester, G. & Zunger, A. Long-and short-range electron-hole exchange interaction in different types of quantum dots. *New J. Phys.* **11,** 123024 (2009).
23. Kowalik, K. *et al.* Monitoring the electrically driven cancellation of exciton fine structure in a semiconductor quantum dot by optical orientation. *Appl. Phys. Lett.* **91,** 183104 (2007).
24. Fry, P. W. *et al.* Inverted Electron-hole alignment in InAs-GaAs self-assembled quantum dots. *Phys. Rev. Lett.* **84,** 733–746 (2000).
25. Langbein, W. *et al.* Control of fine structure splitting and biexciton binding energy in InGaAs quantum dots by annealing. *Phys. Rev. B* **69,** 161301(R) (2004).
26. Bayer, M. *et al.* Fine structure of neutral and charged excitons in self-assembled In(Ga)As/(Al)GaAs quantum dots. *Phys. Rev. B* **65,** 195315 (2002).
27. Tanaka, M., Sakaki, H. & Yoshio, J. Atomic-scale structures of top and bottom heterointerfaces in GaAs-Al$_x$Ga$_{1-x}$As (x=0.2-1) quantum wells prepared by molecular beam epitaxy with growth interruption. *Jpn J. Appl. Phys.* **25,** L155–L158 (1986).
28. Luo, J., Bester, G. & Zunger, A. Atomistic pseudopotential calculations of thickness-fluctuation GaAs quantum dots. *Phys. Rev. B* **79,** 125329 (2009).
29. Hudson, A. J. *et al.* Coherence of an entangled exciton-photon state. *Phys. Rev. Lett.* **99,** 266802 (2007).
30. Kok, P. *et al.* Linear optical quantum computing with photonic qubits. *Rev. Mod. Phys.* **79,** 135–174 (2007).
31. Bluhm, H. *et al.* Dephasing of GaAs electron-spin qubits coupled to a nuclear bath exceeding 200μs. *Nature Phys.* **7,** 109–113 (2010).

Author contributions

M.G. made the device and performed the optical experiments. K.O. carried out the MBE growth of the sample. Y.O. guided the optical measurements. H.O. and K.O. designed the work. All authors analysed the data. All authors contributed to the scientific discussions on the results and commented on the manuscript.

Additional information